Research Square

Preprints are preliminary reports that have not undergone peer review.
They should not be considered conclusive, used to inform clinical practice,
or referenced by the media as validated information.

Spatiotemporal Analysis of Future Drought Vulnerability in the Hindu Kush Region: A Case Study of the Karnali River Basin

Samikshya Hamal
Institute of Engineering
Suraj Lamichhane
klsuraj@gmail.com

Institute of Engineering
Koshish Raj Maharjan
Institute of Engineering

Research Article

Keywords: Karnali River Basin (KRB), Analytical Hierarchy Process (AHP), Geographical Information System (GIS), Drought Vulnerability Map (DVM)

Posted Date: November 10th, 2024

DOI: https://doi.org/10.21203/rs.3.rs-5240619/v1

License: This work is licensed under a Creative Commons Attribution 4.0 International License. Read Full License

Additional Declarations: No competing interests reported.

Version of Record: A version of this preprint was published at Theoretical and Applied Climatology on January 21st, 2025. See the published version at https://doi.org/10.1007/s00704-024-05347-1.

Abstract

A slow-onset catastrophe known as a drought driven by climate change has an impact on the Karnali River Basin, central part of the Himalaya of the Hindu Kush Region. The present study aims to evaluate the spatial and temporal extent and characteristics of the drought using Analytical Hierarchy Process (AHP) in combination with Geographical Information System (GIS) of KRB as this type of research takes less data and resources and can be done using secondary sources data. In addition, this study makes an effort to predict future temperature and precipitation from 2021–2100 utilizing the most recent CMIP6 datasets under two scenarios, SSP245 and SSP585. The majority of highland areas, which comprises as Salyan, Surkhet, and Bardiya from Terai shows the very high vulnerability in every seasons. Central region of Karnali River Basin shows high vulnerability. Pre monsoon, post monsoon, and winter shows the vulnerability ranges from moderate to very high. While the monsoon does not exhibit very high sensitivity meanwhile, the whole KRB exhibits high susceptibility. Under SSP245, coverage of moderate vulnerability is observed to rise during winter and pre monsoon, whereas coverage of high vulnerability is observed to decrease. For instance, moderate vulnerability coverage declines while high vulnerability coverage increases throughout the monsoon and post-monsoon seasons while under SSP585, the vulnerability to winter drought will increase in the future. For the validation of this research, mapping of meteorological drought indices SPI and SPEI have also done, as a result, DVM created by integrating AHP and GIS with less data and secondary data delivers comparable outcomes to real-time data statistics from SPI and SPEI.

INTRODUCTION

Drought is recognized as a severe natural threat having serious consequences for the environment, society, agriculture, and the economy. It is sometimes regarded as a "creeping phenomena," and the effects differ depending on the location (Ekrami et al., 2016). Drought affects food security and wellbeing over a long period of time, unlike other natural dangers, and it operates slowly (V. Pandey et al., 2021). A region's agriculture and water supplies are negatively impacted by drought, one of the worst natural calamities brought on by a lack of water (Kalura et al., 2021). Drought can be generically categorized into four primary types, including hydrological, meteorological, agricultural, and socioeconomic drought, despite the range of definitions (Ha et al., 2022). Meteorological drought results from prolonged periods of insufficient precipitation (Singh & Devi, 2022) resulting in insufficient water levels in lakes, reservoirs, streams (Alharbi et al., 2022), aquatic bodies, and groundwater (Brouziyne et al., 2020) leading to hydrological droughts. An insufficient amount of moisture in the soil at the root zone of plants is known as an agricultural drought (Ha et al., 2022). Socioeconomic drought arises when social production and economic development are negatively impacted by any of these three types of drought (Liang et al., 2021). Unlike other natural disasters like floods, tropical storms, and earthquakes, the effects of drought occur over a wider area, making it especially difficult to estimate their full impact (Boultif & Benmessaoud, 2017). Additionally, droughts can also reduce crop productivity, deteriorate water quality, disrupt riparian habitats, reduce the availability of water, and affect hydropower generation (Singh & Devi, 2022; Thapa et al., 2017). Since drought affects water supplies, such as stream flows, reservoirs, wetlands, and groundwater, it also has a major negative economic impact on non-agricultural industries (Belal et al., 2014).

Droughts have caused severe social, economic, and environmental problems in recent years, including a rise in starvation, an energy crisis, a declines in the volume of water available, and the devastation of habitats (Lweendo et al., 2017). Reduced crop, rangeland, and forest productivity may lead to lower agribusiness profits, higher food and timber prices, jobless rates, and decreased tax receipts due to lower spending, bank loan foreclosures to farmers and businesses, migration, and humanitarian campaigns (Belal et al., 2014). The global economic loss caused by drought-related disasters is estimated to be between $6 and $8 billion annually (Mokarram et al., 2021; Mondol et al., 2017). In the 2015 analysis, Miyan et al. examined the effects of drought on the 14 least developed Asian nations. They discovered that severe droughts are a common occurrence in Bangladesh, Cambodia and Nepal. Among the nation’s most vulnerable to climate change is Nepal (Adhikari, 2018). Many nations have witnessed and identified the consequences of droughts in

recent years. 7.3% of all natural disasters were caused by drought, and its effects are frequently regarded as the most severe (Ha et al., 2022). Recently, a study in the Karnali River Basin of Nepal discovered the occurrence of significant drought events in the following years: 1984–85, 1987–88, 1992–93, 1995–95, 2004–09, and 2012 also revealed a growing frequency of both the monsoon and widespread winter droughts (Khatiwada & Pandey, 2019). Similarly, evaluation of the effects of drought on crop yields through whole Nepal showed the increment of the average number of drought years in the western, central, and eastern regions, respectively, between 1987–2000 and 2001–2017. (Hamal et al., 2020). Winter drought in western Nepal shows increasing tendency over the past 10 years toward more frequent and severe droughts in the dry season (Wang et al., n.d.).

In regard to climate change, it is widely known that there have been numerous instances of extreme drought and heat waves worldwide (V. Pandey et al., 2021), which have placed many nations at risk and had an impact on the hydrological, agricultural, socioeconomic, and meteorological systems (Hamal et al., 2020). A rise in the frequency, severity, and/or quantity of severe weather events such as drought (Lweendo et al., 2017) and heavy precipitation are one of the other signs of global climate change, in addition to rising maritime and land temperatures (Brouziyne et al., 2020). Global warming is expected to produce an increase in the near future in the economic losses resulting from droughts in Asia (Ha et al., 2022). In the Hindu Kush Himalayan (HKH) region, climate change will have varying implications for various sectors such as agriculture, energy and water resources, among others (Wester et al., 2019). The future climate in the Karnali and Mahakali basins in the HKH region will be warmer with higher variability in rainfall dominated by sporadic high intensity rains (V. P. Pandey et al., 2019), additionally according to research based on the IPCC's vulnerability assessment methodology, the KRB and its watersheds are more susceptible to climate change than other significant basins in Nepal (Khatiwada et al., 2016). Droughts and other hydrological extremes have become a significant focus for process study and water resource management strategies; expectations are that climate change will intensify, prolong, and worsen these events (V. Pandey et al., 2021).

Numerous indicators have been proposed to evaluate droughts such as the SPI, SPEI, PDSI, SMI, RDI and SRI that might occur at different time intervals (Nepal et al., 2021; Brouziyne et al., 2020). The complexity of calculation varies among indices, from single input variable for an index such as SPI to two or more variables for SPEI and PDSI, respectively (Lweendo et al., 2017). The ideal strategy to drought management is to implement a complete, cost-effective, and timely drought management system that considers planning for dealing with drought before it occurs and expands. (Ekrami et al., 2016). Vulnerability mapping prepared, integrating GIS with different multi-criteria decision-making methods such as Analytic Hierarchy Process (AHP) Kalura et al., 2021 is crucial for both predicting and preparing for the response to a natural catastrophe making drought evaluation and monitoring easier for users (Singh & Devi, 2022). This is a major reason for most of European, USA and some Asian countries to consider this technique (Ekrami et al., 2016). Various studies have been done to prepare drought sustainability maps using a combination of several criteria, in which proper weights for each criterion have been identified (Mokarram et al., 2021). Central Algeria and East Azarbaijan Province through GIS and multicriteria analysis decision making provided a map of Iran's agricultural drought susceptibility (Ekrami et al., 2016; Karamouz et al., 2015), (Singh & Devi, 2022) identifies drought prone zone in a Low Laying Area, (Alharbi et al., 2022) provided a drought risk map of Kangsabati River Basin, (Palchaudhuri & Biswas, 2016; Kalura et al., 2021; R. P. Pandey et al., 2010) evaluates the spatial extent and characteristics of drought in Puruliya district, Tons River Basin, sonar basin of India, Susceptibility of drought to a region is thus determined by a variety of factors, including topography, soil, usage of land, development of watersheds (irrigation supports), preservation of water, groundwater extractions, and regional demand on water for residential, commercial, and crop production. (R. P. Pandey et al., 2010) This study employs the weighted overlay analysis from ArcGIS to identify a region area that is prone to drought by integrating all of the thematic layers of factors that affects drought in the GIS platform.

Various indices, such as the SPI, SPEI, RDI, SSI, and others (Nepal et al., 2021; Brouziyne et al., 2020), have been used by several countries to detect droughts; however, it requires an extended data set spanning at least 30 years, therefore an

alternative approach to identify drought-prone zones using secondary data through the integration of Geographic Information Systems (GIS) and AHP has been proposed. This study employs the weighted overlay analysis from ArcGIS to identify a region that is prone to drought by integrating all of the thematic layers of factors that affects drought in the GIS platform. This alternative approach requires less observed data and can be performed utilizing secondary sources data.

The primary objective of this study is to evaluate the drought prevalent in Karnali River Basin (KRB) of Nepal. The specific objectives of the present study are:

1. To characterize the historical climatic behavior of KRB.
2. To assess the spatial variability of Drought vulnerability of KRB.
3. To evaluate the impact of climate change on Drought Vulnerability of KRB.

This research aims to identify the drought in present and future scenarios, in terms of spatially and temporally by preparing vulnerability map using an alternative and theoretical approach. The vulnerability map of the drought, indicates whether or not the research region is impacted by drought and, if so, how severely, has been generated by integrating the GIS with AHP. This research addresses drought cohabitation in addition to drought risk and preventing catastrophes. The alternative and theoretical approaches for identifying the drought zones in the region are emphasized in the current study. Drought management requires spatial knowledge on control variables and susceptibility zones. Accurate mapping of drought vulnerability is an effective way for extracting all of this spatial information. Planners and policy makers will find this study beneficial in their adaptation planning, and it may also benefit future academics who wish to expand their research on this river basin.

STUDY AREA

KRB is located in Western Nepal as a part of Himalaya in Hindu Kush Region, with an area exceeding 46,100 km^2, between latitudes 28º20' -30 º 41' N and longitudes 80º33' -83 º 40' E (Fig. 1). From 100 to 7, 721 meters above sea level (masl), the basin's height varies. The longest river in Nepal, the Karnali, rises in China's Tibet to the south of the Mansarovar and Rokas lakes. It meets the Himalayan belt in Nepal at Khojarnath as the Humla-Karnali, one of the numerous snow-fed rivers (Khatiwada & Pandey, 2019). The Terai, Siwalik, Hill, Middle Mountain, and High Mountain physiographic zones of Nepal are all comprised in the basin's area (Shrestha et al., 2022). The six important watersheds are West Seti, Kawadi, Humla Karnali, Mugu Karnali, Tila, and Bheri; Humla Karnali is the only one that originates in China; the other five are all from Nepal. It is intriguing that the Mugu Karnali runs from east to west, and the Humla Karnali from west to east, in contrast to the majority of Nepal's rivers, which typically flow from north to south. The Mahakali River in India, also known as the Ghaghara in the lower regions of the country, is joined by the Karnali River after it flows through western Nepal (Khatiwada et al., 2016).

With significant regional, seasonal, and interannual changes, the basin experiences 1479 mm of precipitation on average annually. With less than 300 mm of precipitation annually, the northern portion of the basin is the driest; yet, some isolated pockets in the hilly regions get more than 2400 mm (Dahal et al., 2020). The summer monsoon season, contributes to 77% of this rainfall, while the winter months, account for just 7%. About 12% of the yearly precipitation occurs during the pre-monsoon period whereas only 4% occurs during the post-monsoon period. Similarly, there are tremendous shifts in the basin's temperature. The basin has an average maximum temperature of 25^oC and an average lowest temperature of approximately 13^oC. With rising altitude, the temperature progressively drops from the south (Terai) to the north (Mountains) (Khatiwada & Pandey, 2019).

METHODOLOGY

Data Collection and Interpretation

The key objectives of this phase are data availability and data preparation for modeling. Results that are reliable are produced by reliable input data. The preparation phase includes the selection of study area, the collection of secondary data from DHM, and data processing where mainly data gap is filled. ArcGIS software, Microsoft Excel, python and R are used to prepare the data. Data from different sources were used to prepare various geospatial layers. These data sources are given in Table 1.

Table 1
Data Type and Data Source

S No	Data Type	Data Source	Resolution
1	Soil Type	Soil and Terrain Database (SOTER)	1:1,000,000
2	Digital Elevation Model (DEM)	Shuttle Radar Topography Mission (SRTM)	30 m
3	Temperature (max, min)	Department of Hydrology and Meteorology (DHM)	Daily
4	Precipitation	Department of Hydrology and Meteorology (DHM)	Daily
5	Land Use Land Cover	International Centre for Integrated Mountain Development (ICIMOD)	30 m

Note: Slope, Aspects and Drainage Density are extracted from DEM using ArcGIS.

Secondary data such as soil type, elevation band, slope, aspects, drainage density, and LULC have been collected from various sources and used to create yearly thematic layers. However, data for precipitation and temperature are aggregated seasonally. Future projection of climate data has been done under two scenarios, the middle of road ideology (SSP2) with the reasonable end of emission scenario (SSP2-4.5) and fossil fueled development ideology with high end emission scenario (SSP5-8.5).The future daily precipitation at 23 stations and temperature at 7 stations respectively has been projected based on an ensemble of five GCMs selected from a pool of 10 CMIP6 GCMs by examining the performance of the CMIP6 models against observed precipitation and temperature data.

The GCMs were compared with the observed data for the baseline period of 1980–2015 with the aim to determine the top 5 among the 10 GCMS. Performance measurements, includes metrics -Nash-Sutcliffe efficiency (NSE), root mean square error (RMSE), and percentage bias (PBIAS). Minimum Temperature has higher ratings, whereas precipitation has lower scores, according to the evaluation performance. The models with the highest scores for precipitation, ranging from 2.07 to 2.16, were EC-Earth3-Veg, MPI-ESM1-2-LR, EC-Earth3, MPI_ESM1-2-HR, and NESM3. Comparably, the greatest ratings for Maximum Temperature were shown by EC-Earth3, NorESM2-LM, NorESM2-MM, EC-Earth3-Veg, and ACCESS-CM2, while the highest ratings for Minimum Temperature were shown by ACCESS-CM2, MRI-ESM2-0, MPI_ESM1-2-HR, MIROC6, and NorESM2-LM, and they ranged from 2.71 to 2.96. Corresponding GCMs have been selected in accordance with their ratings.

Each climate data, Precipitation, Maximum Temperature, Minimum Temperature were Bias Corrected in 13 different quantile mapping methods for Precipitation and 9 for Temperature in R environment. Then bias-corrected GCMs daily data were compared with observed data collected from DHM to calculate three performance metrics NSE, RSR, and PBIAS. The best performing quantile mapping method for a given GCM, has been used on the future time series of the corresponding raw GCMs their ensemble is evaluated for daily precipitation, daily maximum and minimum temperature data. Time series of climate data projection with a daily temporal resolution, at selected meteorological stations, using multi-model ensemble (MME) is the primary output of the downscaling and bias correction process. The projection is

done for three future period, since 2015 to 2100, near-future (NF; 2021–2049), mid-future (MF; 2051–2074), and far future (FF, 2076–2100) for each climate data.

In the current study, effective parameters and factors on meteorological drought vulnerability have been identified. Then, eight parameters were specified as the main indices including Slope, Aspect, Precipitation, Soil Type, Drainage Density, Temperature, LULC and Elevation Band, the indices are classified for weighting and relating to the vulnerability classes by the aid of AHP technique. Classifications of the mentioned indices are performed with the help of international scientific references and local expert knowledge (Ekrami et al., 2016). Each parameter is given a rating, which represents the relative importance of these parameters. Ranking is assigned to each parameter that reflects its importance in the event of occurrence, together with the rating for the individual classes that denotes the event intensity. Figure 2 shows the adopted methodology for this study.

An overview of the selected layers for DVM map

Precipitation and Temperature

Among the parameters compared, rainfall and temperature are the main parameter directly affecting the drought condition of a region. Amount of rainfall and temperature in a region play a significant role in the assessment of drought zones. It is more likely to observe severe drought zones in areas with less rainfall, higher temperatures and high evapotranspiration. On the scale of the impact of drought, the region with high temperatures is assigned a higher rank, and the areas experiencing low temperatures are given a lower rank whereas precipitation has inverse relation, the region with low rainfall is assigned a higher rank and a lower rank to the areas receiving maximum rainfall (Singh & Devi, 2022).

For the precipitation and temperature layer, four seasonal layers for each season—pre-monsoon, monsoon, winter, and post-monsoon have been prepared. The season-specific monthly mean data are first divided, and each seasonal layer is then created in the GIS platform. The final seasonal thematic precipitation layers are created by classifying each layer into five classes using the Natural Breaks tools from the GIS, with 1 denoting very low vulnerability and 5 denoting very high vulnerability, as illustrated in Table 3 and shown in Fig. 3. Using the same methodology, future precipitation and temperature raster are also prepared for NF, MF and FF under SSP245 and SSP585 scenarios.

Soil Type and LULC

In terms of plant and agricultural growth, the interaction between soil and water is crucial. The permeability and water-holding capability of a particular area are significantly influenced by the soil's texture. They are less likely to be hazardous under drought, if the soil type has a strong capacity to preserve or store water. Five categories of landcover are identified in the study: vegetation, agricultural, built-up areas, barren areas, and waterbodies. The LULC maps are generated using supervised classification. In comparison with water bodies, snow, riverbed, (ranked from high to low sensitivity), cropland is more likely to be affected by drought.

Drainage Density

The ratio of a region's total stream channel length to its area is termed as the drainage density. It is a measure of how the river network derived from a digital elevation model (DEM)of 30 m and a kernel density analysis tool of ArcGIS. Areas with higher drainage density tend to have a more developed network of streams and rivers, which can enhance the flow and transport of water during wet periods. On the other hand, regions with lower drainage density have fewer streams and rivers, resulting in slower water movement and reduced water availability during drought conditions.

Elevation Band, Aspects and Slope

The availability of water is also heavily influenced by the plain's elevation. The DEM represents landscapes and ground surface topography and is critical for overcoming problems such as climate change impacts, emergency management, environmental management, and water security. This study has utilized a 30-meter-resolution SRTM DEM dataset (USGS). High elevations are observed in the north region, while the area in the south region is mostly a low-elevation zone as shown in Fig. 3. (Alharbi et al., 2022).

Aspect refers to the slope direction, and different aspects have varying degrees of sun radiation which influence the hydrology of the study area as shown in Fig. 3. This parameter is influenced by hydrology. (Bennie et al. 2008). Different aspects are received different solar radiation levels. Based on the hydrology, this parameter is affected.

Generally, reverse relationship exists between land surface slope and infiltration, where increase in slope would decrease infiltration and vice versa (Ekrami et al., 2016). Slope refers to the inclination or steepness of the land surface in a particular area. However, steep slopes can contribute to the severity and impact of drought in specific areas by influencing water availability, soil moisture content, and vegetation stress.

Ranking of layers are shown in Table 4 and Fig. 4.

AHP Weightage

A Multi-Criteria Decision-Making (MCDM) approach is a pairwise comparison matrix of parameters used to define an objective, is a key component of the AHP technique (Singh & Devi, 2022). The scale factor from 1 to 9, according to importance is shown in Table 2 and is the criterion for evaluating judgment. Pairwise comparisons are used to determine the relative importance with respect to the goal, then normalized the pairwise comparison matrix then calculated the eigen vector. Then performed a consistency check to ensure the validity of the pairwise comparisons. Based on the perspectives of government officials, farmers, and local communities, as well as evaluations of the literature and specialist expertise, these weights have been determined. The final result of the drought zone in ArcGIS is determined by using these weights in the weighted overlay analysis, which additionally considers their degree of impact on the scale (1–5).

Table 2
AHP Description

AHP Description	Intensity of importance Explanation
1	Equally Strong
3	Moderately strong
4	Strongly Strong
7	Very Strongly strong
9	Extremely strong
2,4,6,8	Intermediate values

Following are the formulae, used to determine the consistency ratio (CR) and consistency index (CI):

$$CI = \frac{\max - \mathrm{n}}{n-1}$$

$$CI = \frac{\mathrm{CI}}{CR}$$

where, λmax = maximum eigen value;

n = number of parameters in matrix;

RI = random index value (f orn = 7; RI = 1.32)

Weighted overlay analysis

All eight theme maps in the present model are created using a GIS. The relevant raster maps are subjected to weights from AHP that were used in a GIS model.The weighted overlay method is utilized for the integration of input data layers that is provided in ArcView Model Builder. The total of the accumulated values of all parameters is utilized for the GIS-based classification of drought into several classes after each parameter's rating was multiplied by its weight.

A quick, straightforward, and adequate method for identifying potential drought-threatened regions is the weighted overlay analysis. The research zone was mapped out with regard to drought risk. using eight factors. These factors were ranked numerically proportionally on a scale of 1 to 5, depending on their importance. Higher weights and ranks indicate a bigger influence on the possibility of drought. These elements were combined using the weighted overlay techniques in GIS as thematic layers to produce the drought danger zone map. The drought map was then created by combining all the parameters after multiplying them by the weights assigned to them. The values of the drought map are more significantly affected by the factors with greater weights. Drought map was distinguished into five zones: very high, high, moderate, less and very less drought.

$$D = \sum_{n=1}^{\infty} (Tj\ x\ di)$$

where, Tj expresses the weights of each parameter multiplied to the drought parameters (di)

Table 3
Thematic layers ranking – 1

Precipitation				Temperature				Rank	Vulnerability Class
Pre-Monsoon	Monsoon	Winter	Post-Monsoon	Pre-Monsoon	Monsoon	Winter	Post-Monsoon		
< 70	< 550	< 25	< 2	> 29	> 31	> 21	> 26	5	**Very High**
70 to 110	550 to 700	25 to 30	2 to 4	27 to 29	3. to 31	20 to 21	25 to 26	4	**High**
110 to 170	700 to 800	30 to 40	4 to 6	25 to 27	29 to 30	19 to 20	24 to 25	3	**Moderate**
170 to 240	800 to 950	40 to 45	6 to 8	22 to 25	27 to 29	18 to 19	23 to 24	2	**Less**
> 240	> 950	> 45	> 8	< 22	< 27	< 18	< 23	1	**Very Less**

Table 4: Thematic layers ranking – 2

Soil	LULC	Drainage Density	Slope	Aspects	Elevation Band	Rank	Vulnerability Class
Sandy Soil	Cropland	< 0.3	46 to 83	142 to 215	4777 to 7756	5	**Very High**
Sandy Loam Soil	Bare Slope, Bare Rock	0.3 to 0.5	35.6 to 46	215 to 286	3753 to 4777	4	**High**
Loamy Soil	Forest, Grassland	0.5 to 0.6	26 to 35.6	68.4 to 142	2619 to 3753	3	**Moderate**
Sandy Clay Loam	Build Up Area	0.6 to 0.8	14.3 to 26	286 to 360	1522 to 2619	2	**Less**
Ice and Glacier	Water Body, Snow and Glacier, Riverbed	> 0.8	0 to 14.3	1 to 68.4	141 to 1522	1	**Very Less**

RESULTS AND DISCUSSION

As can be seen in Fig. 5, during the Winter, apart from Jumla, the entire KRB is vulnerable from moderate to very high. The region between Siwalik to the Moutain is highly vulnerable with few scattered areas having very high vulnerability. Based on the statistical analysis, 39% of KRB is impacted by high vulnerability, while 55% of area coverage is moderate vulnerability, dominating the entire KRB. As it reaches Pre-Monsoon, whole KRB is vulnerable with region moving from east to west, showing the less vulnerability to high vulnerability. As season approaches Pre-Monsoon, the entire KRB becomes vulnerable, with regions spanning from east to west experiencing moderate to very high vulnerabilities. Pre-monsoon DVM demonstrates that high vulnerability covers 48% of the area and 49% of region is occupied by moderate vulnerability. Despite the fact that rainfall occurs frequently throughout the Monsoon season, KRB continues to be a drought-prone area with moderate to high vulnerability.Monsoon DVM demonstrates that 26% of the region is occupied by high vulnerability and 73% of the region encompassed by moderate vulnerability dominating entire KRB. KRB is heavily affected with high and very high vulnerability during Post-Monsoon from the central-west region, only the eastern side experiences moderate drought and only a very small area is less vulnerable. The KRB is dominated by moderate vulnerability, however among all seasons combined, Post Monsoon DVM has the highest coverage of very high vulnerability of 4%.

Meteorological Drought Mapping

Validation of DVM with Meteorological Drought Indices

To validate the Meteorological drought vulnerability map prepared through the integration of AHP and GIS, meteorological drought indices are calculated. In this research work, Standardized Precipitation Index (SPI) and Standardized Precipitation Evapotranspiration Index (SPEI) are used as, these indices are used to quantify drought has been attributed to their global reputation as the finest indicators for meteorological drought detection. The SPI and SPEI indices are calculated over various time scales: 1, 2, 3, 4, 6 and 12-months. Different time scales indices have been used for different seasons, attempting to obtain meteorological seasonal drought mapping. Using the concept of runs theory, Total Drought Severity (TDS) and Total Drought Duration (TDD) for each season are calculated and using the IDW in GIS platform, meteorological drought mapping are achieved.

Figure 6 and 7 shows the TDD and TDS mapping of SPI and SPEI statistics. TDD during winter from both SPI and SPEI shows highest no of duration occurrence and highest severity is in terai to Himalayan's from central to western KRB. Highest TDS and TDD from SPI is observed in Achham, Kalikot, Surkhet, Bardiya whereas TDS and TDD from SPEI is observed in Dailekh, Jajarkot, Surkhet and Bardiya. Almost every KRB region has suffered from drought at some point

over the winter. During the pre- monsoon, according to SPI statistics, Western KRB and other scattered areas like Bajhang, Doti, Kalikot, Surkhet, Jajarkot experienced the largest number of drought occurrences and severity. According to SPEI Doti, Surkhet, Kailali, Bardiya, Jumla, Mugu and other western district shows the longest Drought duration and highest severity. During the monsoon, SPI with the exception of Mugu and Surkhet, entire KRB, mostly mountainous region shows the longest drought occurrence and highest severity. While the rest of the KRB exhibits the maximum severity, SPEI indicates that the western KRB has the least amount of drought, although this being the longest season overall. While monsoon contributes the highest rainfall of all the seasons, however, TDD and TDS in KRB are also highest during monsoon, according to SPEI statistics. During Post-Monsoon, according to SPI statistics, eastern KRB shows highest occurrence of drought along with highest severity with few districts like Doti, Bajhang from west. Meanwhile, according to SPEI statistics, western KRB shows the highest severity with longest drought and less TDD and TDS is observed in eastern KRB. During Post- Monsoon SPI and SPEI exhibits opposing outcomes.

When comparing DVM statistics with SPI and SPEI, SPEI outperforms SPI. Due to the fact that, precipitation is the only factor that determines SPI whereas SPEI is a function of both precipitation and temperature, and since precipitation and temperature carried the greatest weight in the DVM, the results of SPEI statistics and DVM are comparable. Aside from this study, previous studies and other research work also suggest the increment in temperature and reduction in rainfall, which is, by definition, the primary cause of Meteorological Drought. Few research papers on Nepalese drought identification suggest that the western region of Nepal experiences the most drought. Furthermore, DVM created by integrating AHP and GIS with less data and secondary data delivers comparable outcomes to real-time data statistics from SPI and SPEI. As a result, it can be performed quicker with less data available and by utilizing secondary data, making it helpful for identifying droughts.

Future DVM map

Future Winter DVM under SSP245 & SSP585 for NF, MF & FF

As shown in Fig. 8, Future winter drought is expected to affect the East to central KRB with high to very high vulnerability while western KRB shows vulnerability ranging from less to moderate in all NF, MF and FF under both SSP245 and SSP585. NF under both SSP245 and SSP585 shows very high vulnerability in Jajarkot and Salyan, whereas in MF and FF under both SSP245 and SSP585 shows very high vulnerability in Jajarkot, Salyan and Surkhet.

The percentage of moderately vulnerable areas under SSP245 decreases from 55 to 53 as they proceed from NF to MF and rises to 71 as they reach FF, while the percentage of highly vulnerable areas rises to 43 from 38 as they proceed from NF to MF and drops to 22 as they reach FF. Very high vulnerability exhibits an increasing order as it moves from NF to MF to FF, from 1 to 2 and to 3. Under SSP585, the percentage of area of moderate vulnerability rises slightly from 53 to 54 as it proceeds from NF to MF and reduces to 48 as it arrives at FF, whereas area of high vulnerability decreases to 37 from 44 as it proceeds from NF to MF and rises to 48 as it reaches FF. Very high vulnerability increases from 1 to 3 as it arrives at MF and reduces to 2 as it enters FF.

Future Pre-Monsoon DVM under SSP245 & SSP585 for NF, MF & FF

Post monsoon drought from Fig. 9, shows the inconsistent pattern in different future periods. Entire KRB shows the vulnerability ranging from moderate to very high, while very high vulnerability being common in districts Surkhet, Jajrakot and Salyan. Western KRB shows high and very high vulnerability during NF and FF SSP245. High vulnerability is observed in central KRB during NF in eastern KRB during MF and FF under SSP585.

The percentage of moderately vulnerable areas under SSP245 increases from 51 to 70 as they proceed from NF to MF and falls to 54 as they reach FF, while the percentage of highly vulnerable areas drops to 26 from 45 as they proceed from NF to MF and rises to 41 as they reach FF. Very high vulnerability exhibits an increasing order as it moves from NF to MF

and FF, from 1 to 2. Under SSP585, the percentage of area of moderate vulnerability rises slightly from 53 to 54 as it proceeds from NF to MF and reduces to 48 as it arrives at FF, whereas area of high vulnerability decreases to 37 from 44 as it proceeds from NF to MF and rises to 48 as it reaches FF. Very high vulnerability increases from 1 to 3 as it arrives at MF and reduces to 2 as it enters FF.

Future Monsoon DVM under SSP245 & SSP585 for NF, MF & FF

As shown in Fig. 10, Future monsoon drought shows, entire KRB is vulnerable to drought with high vulnerability dominating the entire basin in all future under both SSP245 and SSP585. Only in FF under SSP585, moderate vulnerability is predicted to dominate KRB. Very high vulnerability is observed in few areas of Jajarkot and Salyan.

The percentage of moderately vulnerable areas under SSP245 increases from 41 to 56 as they proceed from NF to MF and decreases to 29 as they reach FF, while the percentage of highly vulnerable areas drops to 42 from 57 as they proceed from NF to MF and rises to 69 as they reach FF. Under SSP585, the percentage of area of moderate vulnerability falls slightly 31 to 28 as it proceeds from NF to MF and heavily rises to 58 as it arrives at FF, whereas area of high vulnerability slightly rises to 70 from 68 as it proceeds from NF to MF and falls to 40 as it reaches FF.

Future Post-Monsoon DVM under SSP245 & SSP585 for NF, MF & FF

As shown in Fig. 11, Central KRB is estimated to highly affected in all future periods under both scenarios SSP245 and SSP585. NF and MF under SSP245 shows the largest vulnerability in almost entire KRB. FF under SSP245 and NF under SSP585, shows more vulnerability in eastern KRB. Similarly, MF and FF under SSP585 shows scattered high vulnerability in both eastern and western KRB.

The percentage of moderately vulnerable areas under SSP245 shows increasing tendency, where it rises from 41 to 47 and to 59 as they proceed from NF to MF and to FF, while the percentage of highly vulnerable areas shows decreasing, where it falls from 57 to 50 to 38 as they proceed from NF to MF and to FF. Very high vulnerability exhibits an increasing order as it moves from NF to MF to FF, from 0 to 1. Under SSP585, the percentage of area of moderate vulnerability rises slightly from 49 to 53 as it proceeds from NF to MF and slightly reduces to 52 as it arrives at FF, whereas area of high vulnerability shows ranges around 44 in all Future periods.

Comparison of Historical with SSP245

As shown in Fig. 12, percentage of area in winter Drought vulnerability is historically similar to NF and MF, however it has been observed to vary in FF. The domain of moderate vulnerability is the same for historical and NF, decreasing by 2% as it reaches MF but growing rapidly to 71% as it reaches FF. The area of high vulnerability decreases by 1% and increases by 4% as it undergoes NF and FF, but falls to 22% as it reaches FF. Very high vulnerability it rises to 1%, 2%, and 3% as it approaches NF, MF, and FF. The percentage of pre-monsoon drought vulnerability in historical statistics shows a similar pattern for NF and FF, however significant variations are observed for MF. During historical, NF, and FF, areas of moderate vulnerability and high vulnerability ranged between 50% and 45%, respectively. Moderate vulnerability grows to 70% and then falls to 26% when MF arrives. Very high vulnerability exhibits an increasing tendency, with the proportion of land covered increasing to 2% as it progresses from historical to NF and then to 3% as it reaches MF and FF levels.

The percentage of areas vulnerable to Monsoon moderate drought reduces to 41%, 56%, and 29% from 73% in future periods NF, MF, and FF, respectively, from historical periods. As it approaches NF, MF, and FF, high vulnerability rises to 57%, 42%, and 69%, respectively, compared with 26% previously. During the monsoon season, there is no evidence of very high susceptibility. The percentage of areas with moderate susceptibility decreases while the percentage of areas with high vulnerability increases over time. Moderate vulnerability reduces from 66–41%, 47%, and 59%, respectively, when it transitions from historical to NF, MF, and FF. As time proceed from historical to future periods, high vulnerability rises

from 27–57%, 50%, and 38%, respectively. Very high vulnerability exhibits a decreasing trend, with a drop to 1% in future periods.

Based on this, it can be concluded that coverage of moderate vulnerability is observed to rise during winter and pre monsoon, whereas coverage of high vulnerability is observed to decrease. For instance, moderate vulnerability coverage declines while high vulnerability coverage increases throughout the monsoon and post-monsoon seasons. Future periods simultaneously show very high susceptibility. Drought is observed in all seasons and future periods, despite the fact that drought vulnerability varies between drought classes.

Comparison of Historical with SSP585

As shown in Fig. 13, the historical winter drought vulnerability percentage is comparable to that of NF, MF, and FF, where the percentage of high vulnerability is approximately 40% and the percentage of moderate vulnerability is approximately 50%. Very high vulnerability, which spans 1% in NF, 3% in MF, and 2% in FF, exhibits an increasing tendency. The percentage of coverage area in NF that is vulnerable to the pre-monsoon drought is comparable to previous periods, with the exception of very high vulnerability, which accounts for 5% of the total. The coverage of moderate vulnerability elevates quickly to 74% and 63% as it approaches MF and FF, while the coverage of high vulnerability falls to 20% and 24% as it approaches MF and FF. Very high vulnerability coverage is 1% in historical data, but increases to 5% in NF and 6% in FF. As it approaches MF and FF, the covering area of reduced vulnerability likewise expands to 4% and 5%, respectively.

Future periods are observed to experience an increase in monsoon vulnerability. In NF, MF, and FF, area coverage of high vulnerability rises from 26–68%, 70%, and 40%, while area coverage of moderate vulnerability falls from 73–31%, 28%, and 58%. Likewise, future periods are also observed to experience an increase in post-monsoon vulnerability. In NF, MF, and FF, area coverage of high vulnerability rises from 27–44%, 44%, and 45%, whereas area coverage of moderate vulnerability falls from 66–49%, 53%, and 52%. Based on the increasing high vulnerability, it is possibly specified that the vulnerability to winter drought will increase in the future. The KRB as a whole is dominated by moderate vulnerability due to the pre-monsoon drought. The monsoon season has the highest level of vulnerability, and it will only get stronger with time. Additionally, the post-monsoon period demonstrates a future with growing high vulnerability. Future drought vulnerability under SSP585 illustrates the trend toward increased drought severeness.

CONCLUSIONS

This study presents the spatial and temporal evolution of drought in the KRB, the central part of the Himalaya of Hindu Kush Region. The Precipitation trend in KRB shows decreasing tendency whereas Temperature trend shows increasing tendency which is the main cause of meteorological drought hence, KRB is climatically more sensitive to drought. Basically, mountain regions are most fragile, and western KRB is more sensitive than eastern KRB. Entire KRB shows the vulnerability ranging from moderate to very high throughout the year. The majority of highland areas, which comprises as Bardiya, Salyan, Surkhet, and Bardiya from Terai shows the very high vulnerability in every seasons. Central region of KRB from terai to high Himalayan shows high vulnerability. Winter, Pre-Monsoon and Post Monsoon shows the vulnerability ranges from moderate to very high. While the monsoon does not exhibit extremely high sensitivity meanwhile, the whole KRB exhibits high susceptibility. The impacted region has the biggest percentage shift in NF and FF under SSP585 during the pre-monsoon, with VH vulnerability reaching 5% and 6%, respectively. The percentage of the KRB that is dominated by high vulnerability is observed in the following areas: NF (57%), FF (69%) of the monsoon, NF (57%), MF (50%) of the post-monsoon under SSP245 and similarly in NF (68%) and MF (70%) of the monsoon under SSP 585.

Using an integrated approach of GIS and AHP technique this research attempts to provide an alternate technique of identifying drought regions when time and resources are limited. With pairwise comparison matrix among the parameters, help in ranking those parameters for the identification of drought zones, and its normalized weights, which effectively address the hierarchical relationships among the parameters, the AHP method has made it easier to assess

the drought regions. The majority of the regions in the KRB can be classified as highly vulnerable, referring to the meteorological vulnerability map. Only alternate and straightforward approaches for identifying the region's drought zones are highlighted in this study. This study has demonstrated the great potential of GIS combined with the AHP approach for determining drought zones in the area. This theoretical approach, with less information and in a very short period of time, drought assessment can be done and gives acceptable result. As a result, policymakers and decision-makers can respond quickly and effectively to any drought situation.

Declarations

Author Contribution

SH performed major analysis and was a major contributor in writing the manuscript.SL supervised the entire work , reviewed the manuscript.KRM assisted in data preparation and analysis.All authors contributed to the study conception and design. All authors read and approved the final manuscript.

Data Availability

Data is provided within the manuscript or supplementary information files.

References

1. Adhikari S (2018) Drought impact and adaptation strategies in the mid-hill farming system of western nepal. In *Environments - MDPI* (Vol. 5, Issue 9, pp. 1–12). MDPI AG. https://doi.org/10.3390/environments5090101
2. Alharbi RS, Nath S, Faizan OM, Hasan MSU, Alam S, Khan MA, Bakshi S, Sahana M, Saif MM (2022) Assessment of Drought vulnerability through an integrated approach using AHP and Geoinformatics in the Kangsabati River Basin. J King Saud Univ - Sci 34(8):102332. https://doi.org/10.1016/j.jksus.2022.102332
3. Belal AA, El-Ramady HR, Mohamed ES, Saleh AM (2014) Drought risk assessment using remote sensing and GIS techniques. Arab J Geosci 7(1):35–53. https://doi.org/10.1007/s12517-012-0707-2
4. Boultif M, Benmessaoud H (2017) Using climate-soil-socioeconomic parameters for a drought vulnerability assessment in a semi-arid region: Application at the region of El Hodna, (M'sila, Algeria). Geogr Pannonica 21(3):142–150. https://doi.org/10.5937/GeoPan1703142B
5. Brouziyne Y, Abouabdillah A, Chehbouni A, Hanich L, Bergaoui K, McDonnell R, Benaabidate L (2020) Assessing hydrological vulnerability to future droughts in a Mediterranean watershed: Combined indices-based and distributed modeling approaches. Water (Switzerland) 12(9). https://doi.org/10.3390/W12092333
6. Dahal P, Shrestha ML, Panthi J, Pradhananga D (2020) Modeling the future impacts of climate change on water availability in the Karnali River Basin of Nepal Himalaya. Environ Res 185(February):109430. https://doi.org/10.1016/j.envres.2020.109430
7. Ekrami M, Marj AF, Barkhordari J, Dashtakian K (2016) Drought vulnerability mapping using AHP method in arid and semiarid areas: a case study for Taft Township, Yazd Province, Iran. Environ Earth Sci 75(12):1039. https://doi.org/10.1007/s12665-016-5822-z
8. Ha TV, Huth J, Bachofer F, Kuenzer C (2022) A Review of Earth Observation-Based Drought Studies in Southeast Asia. In *Remote Sensing* (Vol. 14, Issue 15). MDPI. https://doi.org/10.3390/rs14153763
9. Hamal K, Sharma S, Khadka N, Haile GG, Joshi BB, Xu T, Dawadi B (2020) Assessment of drought impacts on crop yields across Nepal during 1987–2017. Meteorol Appl 27(5). https://doi.org/10.1002/met.1950

10. Kalura P, Pandey A, Chowdary VM, Raju PV (2021) Assessment of Hydrological Drought Vulnerability using Geospatial Techniques in the Tons River Basin, India. J Indian Soc Remote Sens 49(11):2623–2637. https://doi.org/10.1007/s12524-021-01413-7
11. Khatiwada KR, Pandey VP (2019) Characterization of hydro-meteorological drought in Nepal Himalaya: A case of Karnali River Basin. *Weather and Climate Extremes*, *26*. https://doi.org/10.1016/j.wace.2019.100239
12. Khatiwada KR, Panthi J, Shrestha ML, Nepal S (2016) Hydro-climatic variability in the Karnali River Basin of Nepal Himalaya. Climate 4(2):1–14. https://doi.org/10.3390/cli4020017
13. Liang Z, Su X, Feng K (2021) Drought propagation and construction of a comprehensive drought index based on the Soil and Water Assessment Tool (SWAT) and empirical Kendall distribution function (*K*C'): A case study for the Jinta River basin in northwestern China. Nat Hazards Earth Syst Sci 21(4):1323–1335. https://doi.org/10.5194/nhess-21-1323-2021
14. Lweendo MK, Lu B, Wang M, Zhang H, Xu W (2017) Characterization of droughts in humid subtropical region, upper kafue river basin (Southern Africa). Water (Switzerland) 9(4):242. https://doi.org/10.3390/w9040242
15. Mokarram M, Pourghasemi HR, Hu M, Zhang H (2021) Determining and forecasting drought susceptibility in southwestern Iran using multi-criteria decision-making (MCDM) coupled with CA-Markov model. Sci Total Environ 781:146703. https://doi.org/10.1016/j.scitotenv.2021.146703
16. Mondol MAH, Ara I, Das SC (2017) Meteorological Drought Index Mapping in Bangladesh Using Standardized Precipitation Index during 1981–2010. *Advances in Meteorology*, *2017*. https://doi.org/10.1155/2017/4642060
17. Nepal S, Pradhananga S, Kumar Shrestha N, Kralisch S, Shrestha JP, Fink M (2021) Space-time variability in soil moisture droughts in the Himalayan region. Hydrol Earth Syst Sci 25(4):1761–1783. https://doi.org/10.5194/hess-25-1761-2021
18. Palchaudhuri M, Biswas S (2016) Application of AHP with GIS in drought risk assessment for Puruliya district, India. Nat Hazards 84(3):1905–1920. https://doi.org/10.1007/s11069-016-2526-3
19. Pandey RP, Pandey A, Galkate RV, Byun HR, Mal BC (2010) Integrating Hydro-Meteorological and Physiographic Factors for Assessment of Vulnerability to Drought. Water Resour Manage 24(15):4199–4217. https://doi.org/10.1007/s11269-010-9653-5
20. Pandey VP, Sharma A, Dhaubanjar S, Bharati L, Joshi IR (2019) Climate shocks and responses in Karnali-Mahakali Basins, Western Nepal. Climate 7(7). https://doi.org/10.3390/CLI7070092
21. Pandey V, Srivastava PK, Singh SK, Petropoulos GP, Mall RK (2021) Drought identification and trend analysis using long-term chirps satellite precipitation product in bundelkhand, india. Sustain (Switzerland) 13(3):1–20. https://doi.org/10.3390/su13031042
22. Shrestha B, Zhang L, Sharma S, Shrestha S, Khadka N (2022) Effects on ecosystem services value due to land use and land cover change (1990–2020) in the transboundary Karnali River Basin, Central Himalayas. SN Appl Sci 4(5). https://doi.org/10.1007/s42452-022-05022-y
23. Singh NM, Devi TT (2022) Assessment and Identification of drought prone zone in a Low Laying Area by AHP and MIF method: A GIS based study. *IOP Conference Series: Earth and Environmental Science*, *1084*(1). https://doi.org/10.1088/1755-1315/1084/1/012047
24. Thapa BR, Ishidaira H, Pandey VP, Shakya NM (2017) A multi-model approach for analyzing water balance dynamics in Kathmandu Valley, Nepal. J Hydrology: Reg Stud 9:149–162. https://doi.org/10.1016/j.ejrh.2016.12.080
25. Wang S-Y, Yoon J-H, Gillies RR (n.d). What Caused Winter Drought Western Nepal Dur Recent Years? https://doi.org/10.1175/JCLI-D
26. Wester P, Mishra A, Mukherji A, Shrestha AB, Change C (2019) The Hindu Kush Himalaya Assessment. In *The Hindu Kush Himalaya Assessment*. https://doi.org/10.1007/978-3-319-92288-1

Figures

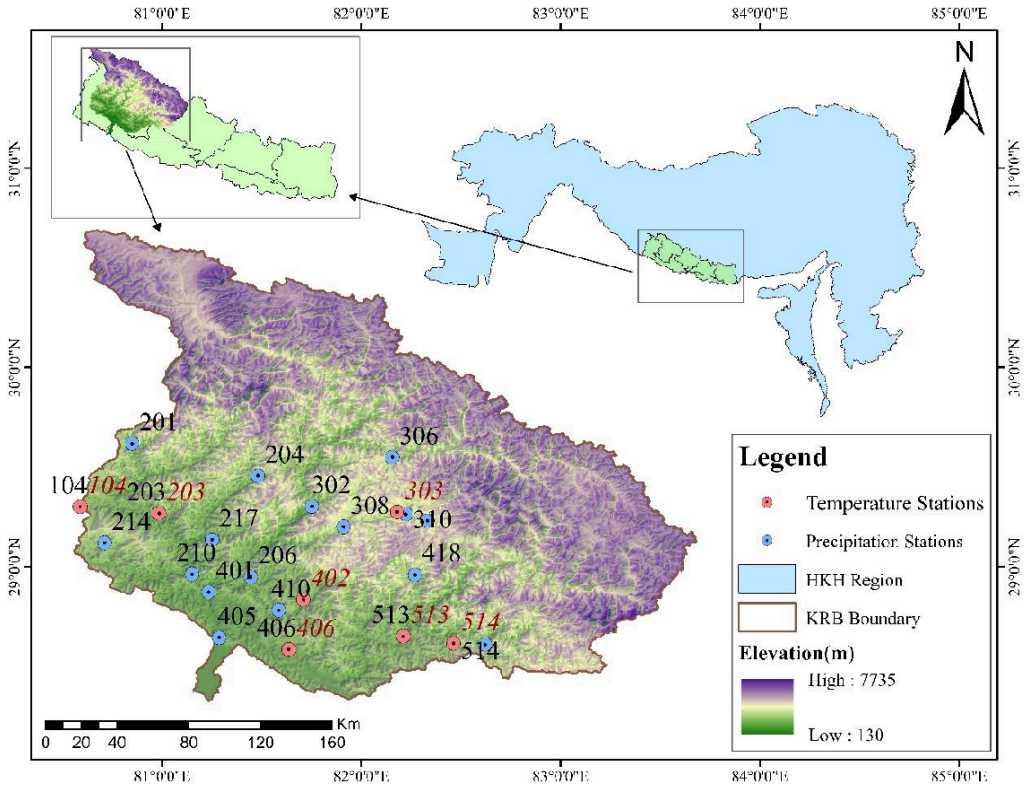


Figure 1: Karnali River Basin

Figure 1

See image above for figure legend

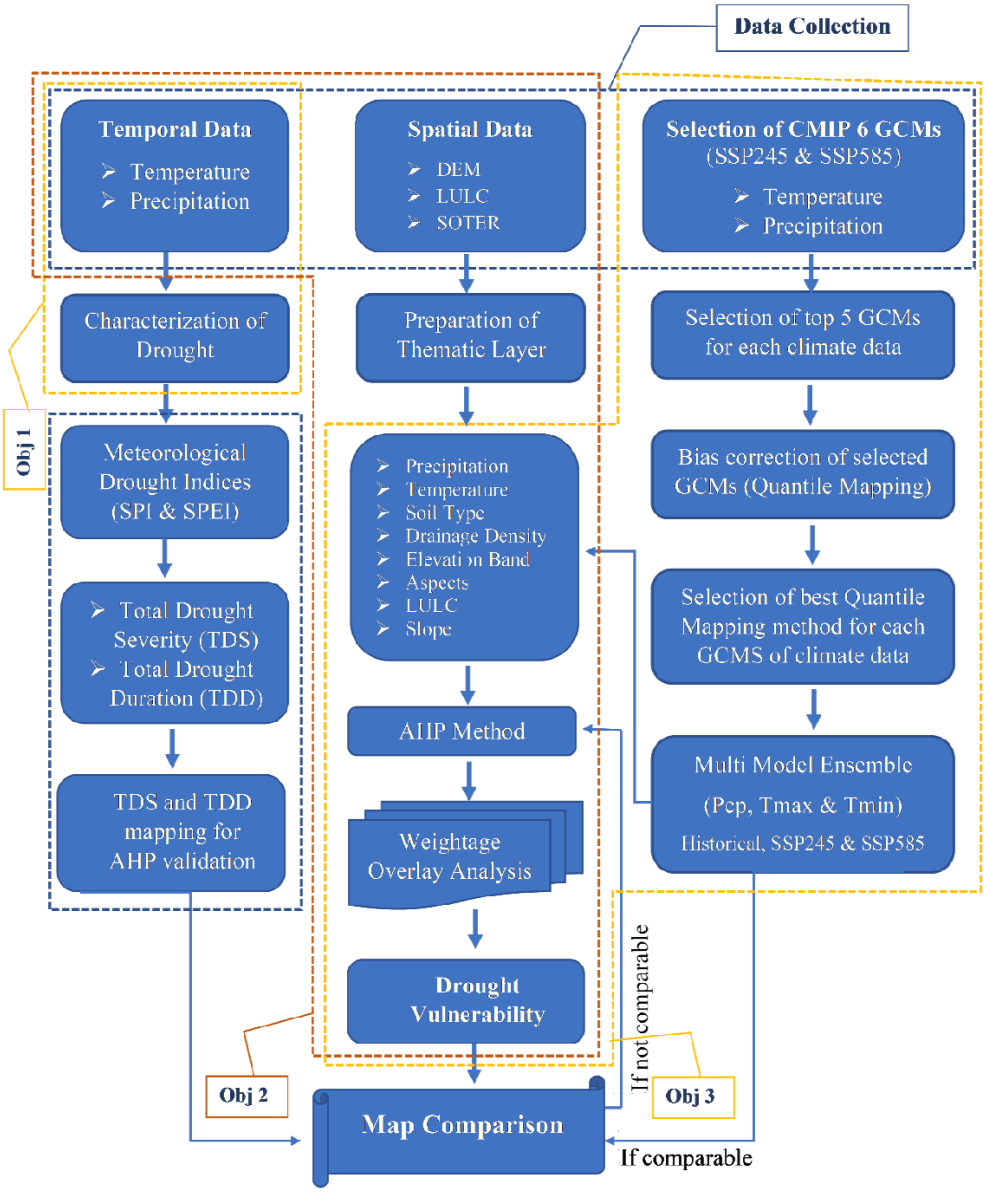


Figure 2: Conceptual Framework for Drought Assessment

Figure 2

See image above for figure legend

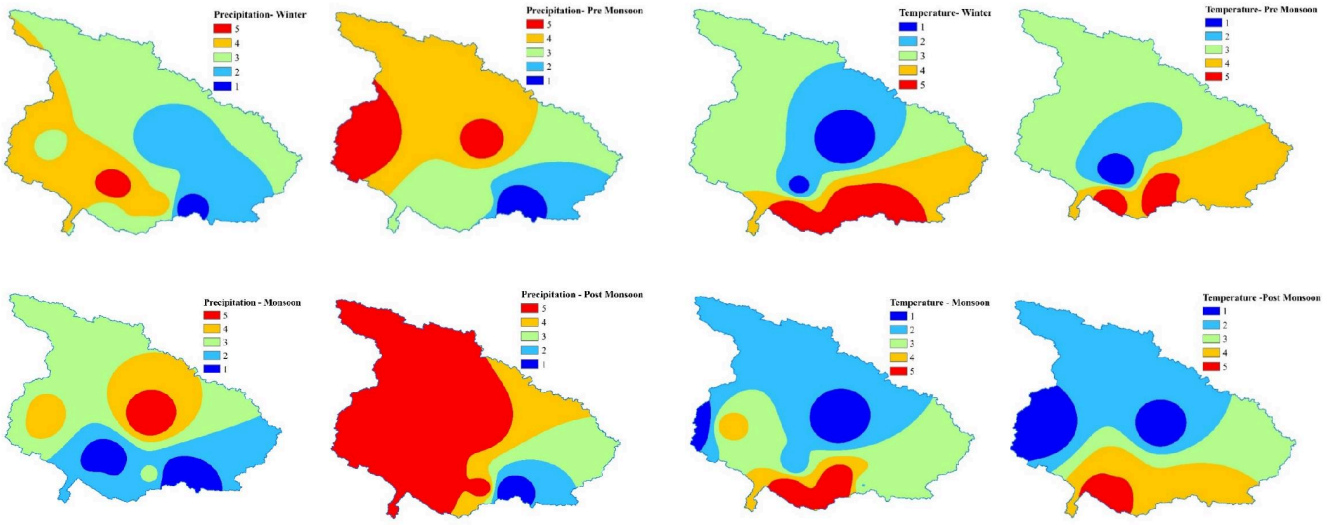


Figure-3: Seasonal Precipitation and Temperature thematic layer

Figure 3

See image above for figure legend

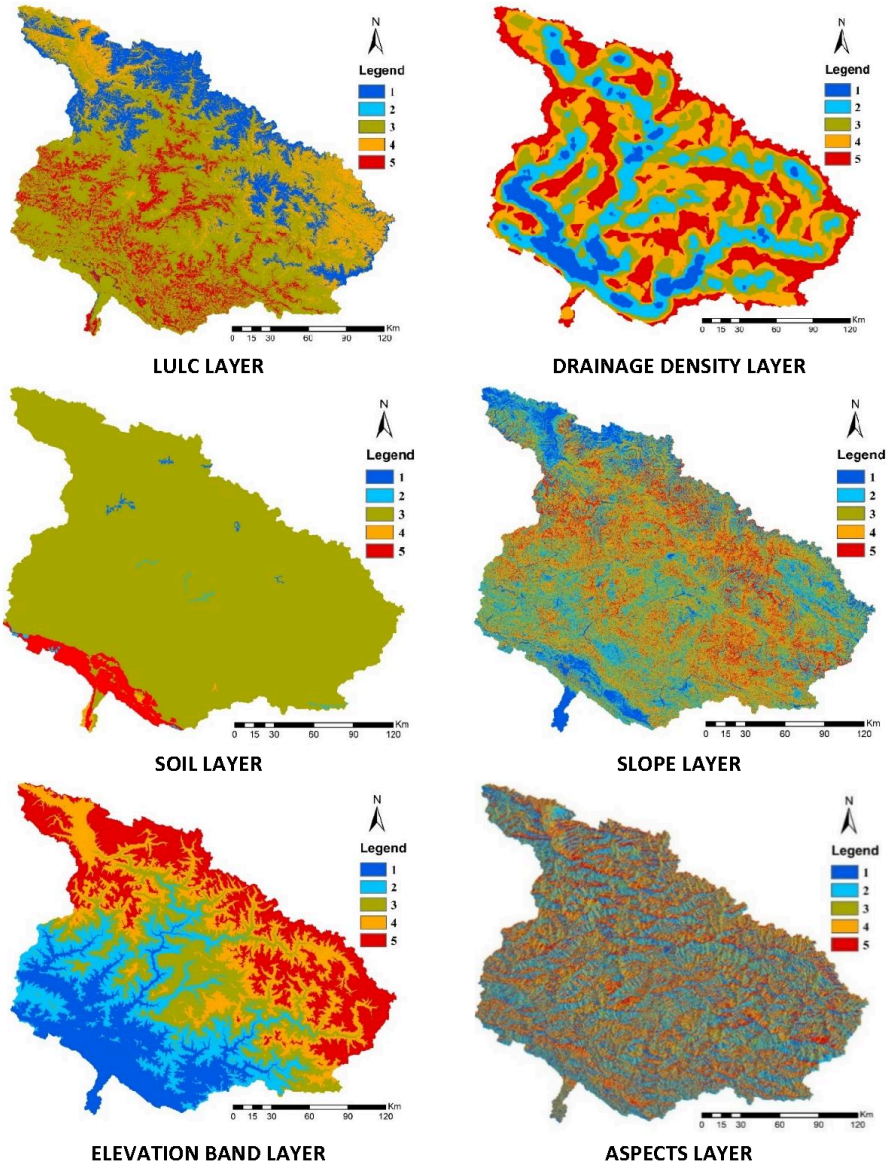


Fig 4- Thematic Layers

Figure 4

See image above for figure legend

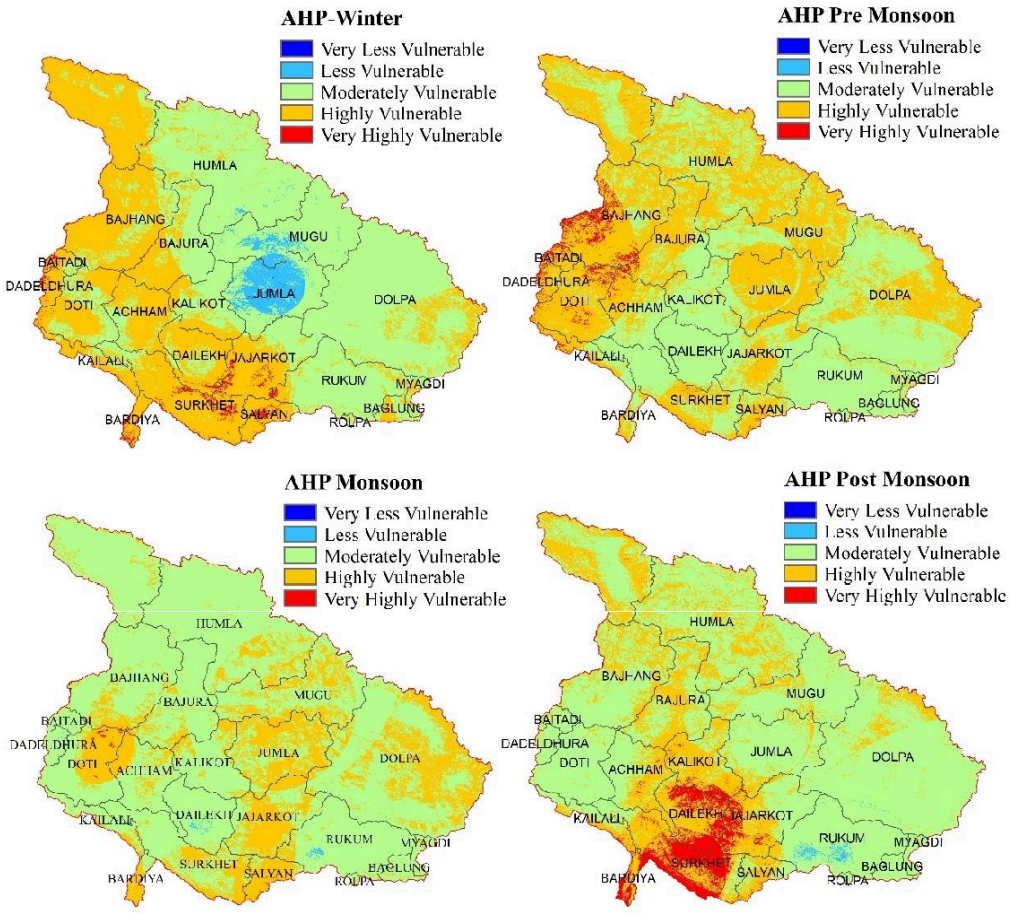


Figure 5: Seasonal Drought Vulnerability Map of KRB

Figure 5

See image above for figure legend

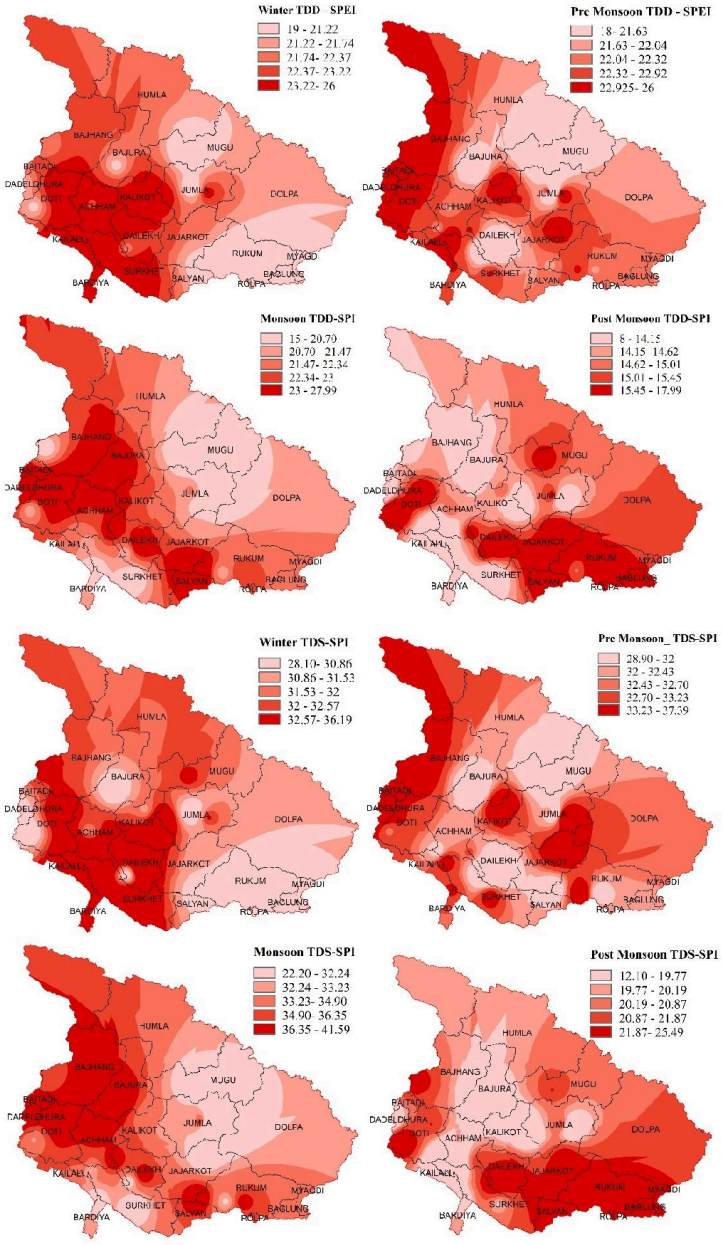


Figure 6: TDD & TDS- SPI Mapping

Figure 6

See image above for figure legend

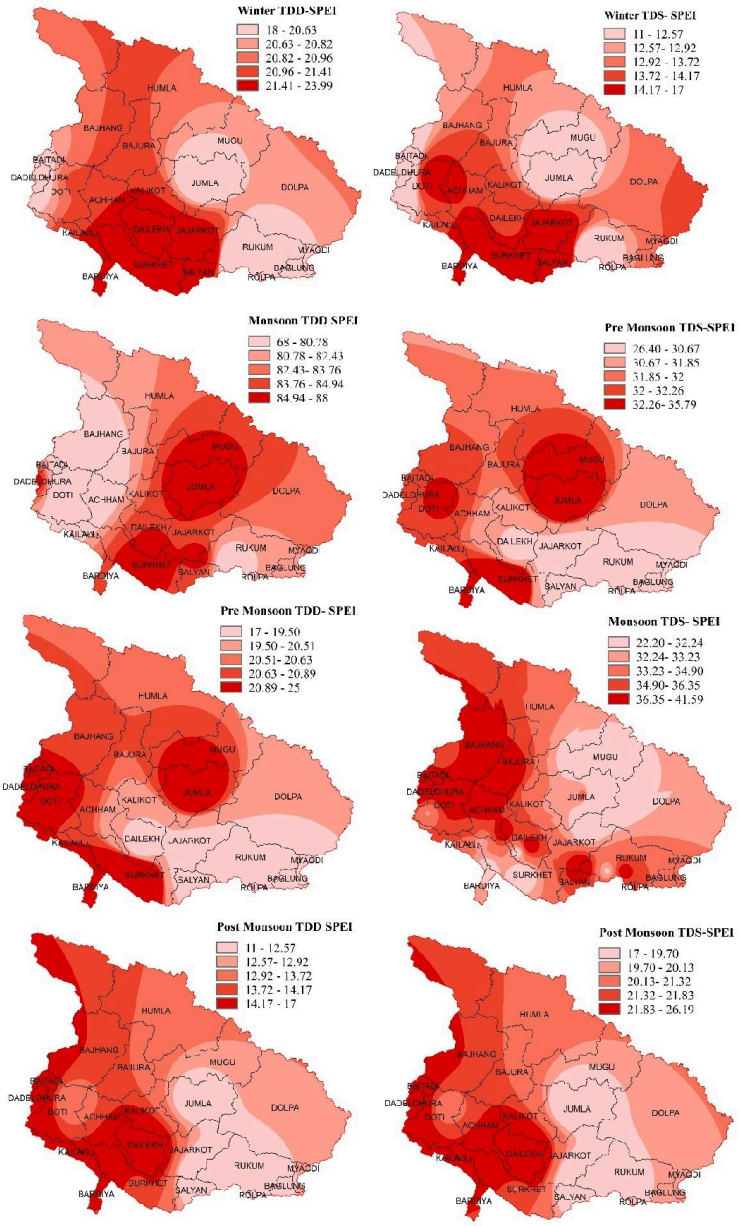


Figure 7: TDD & TDS- SPEI Mapping

Figure 7

See image above for figure legend

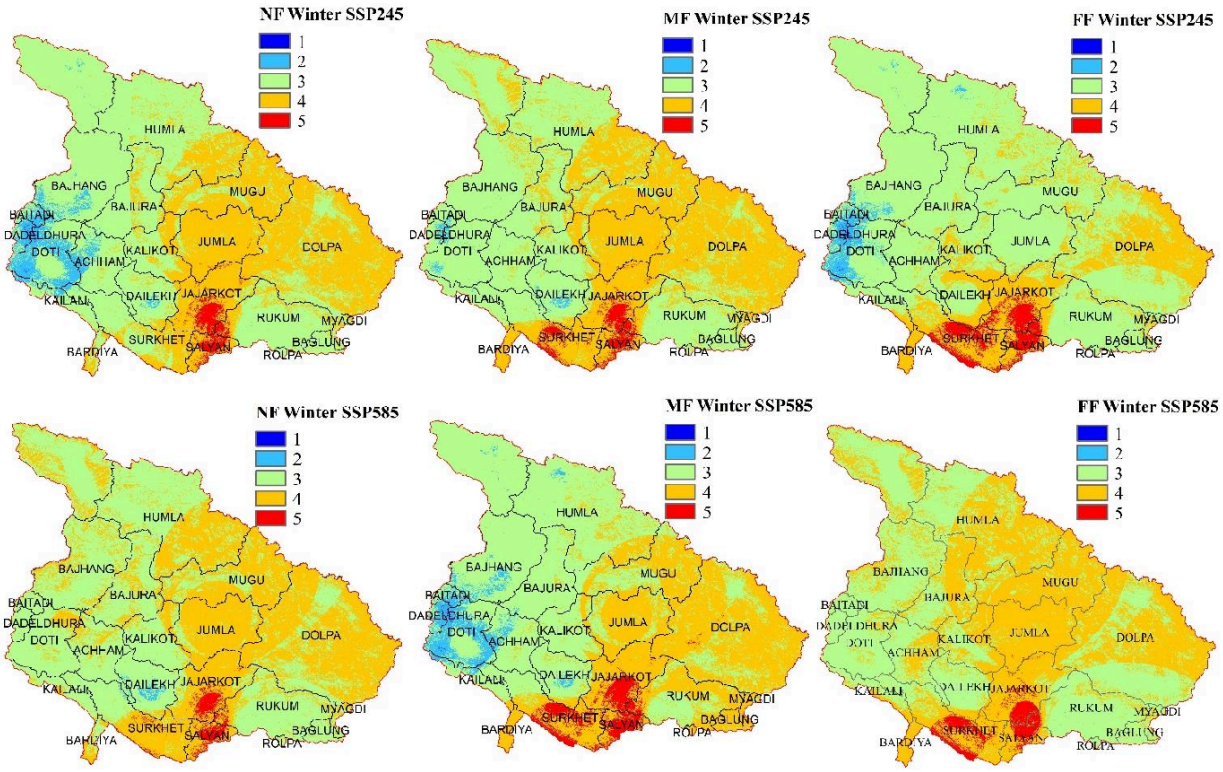


Figure 8: Future Winter DVM under SSP245 & SSP585 for NF, MF and FF

Figure 8

See image above for figure legend

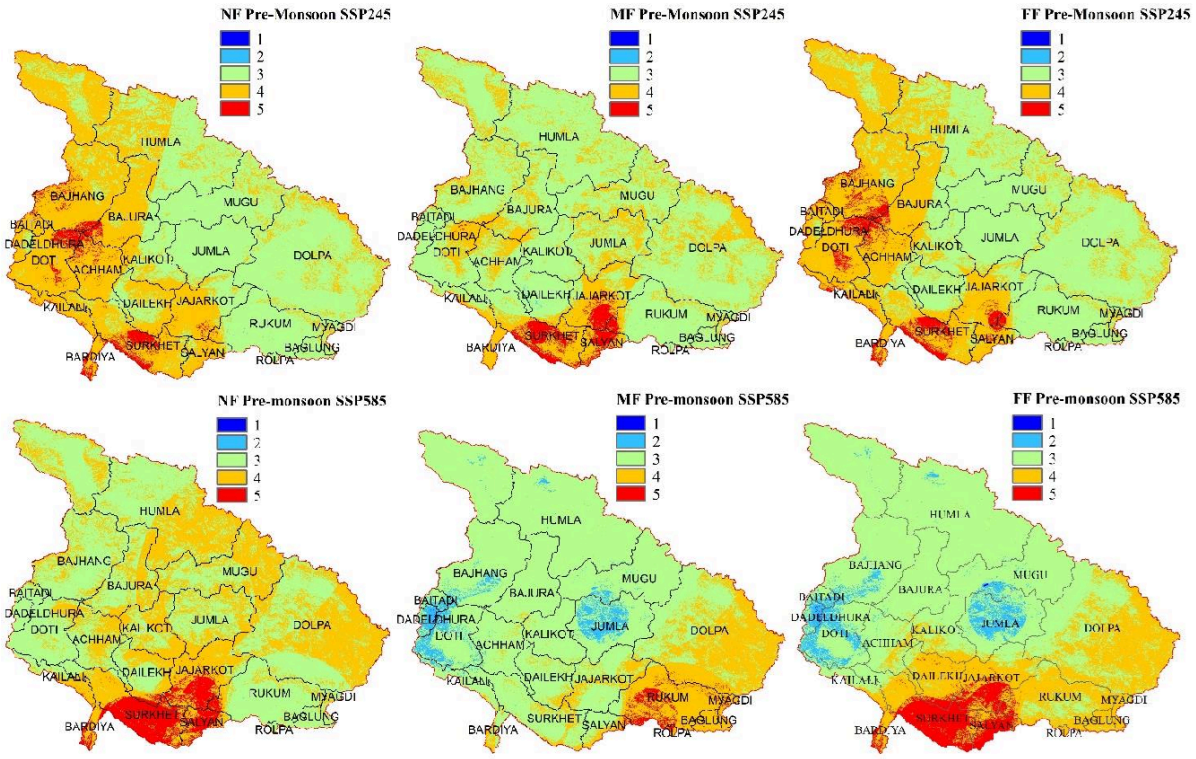


Figure 9: Pre-Monsoon DVM under SSP245 & SSP585 for NF, MF and FF

Figure 9

See image above for figure legend

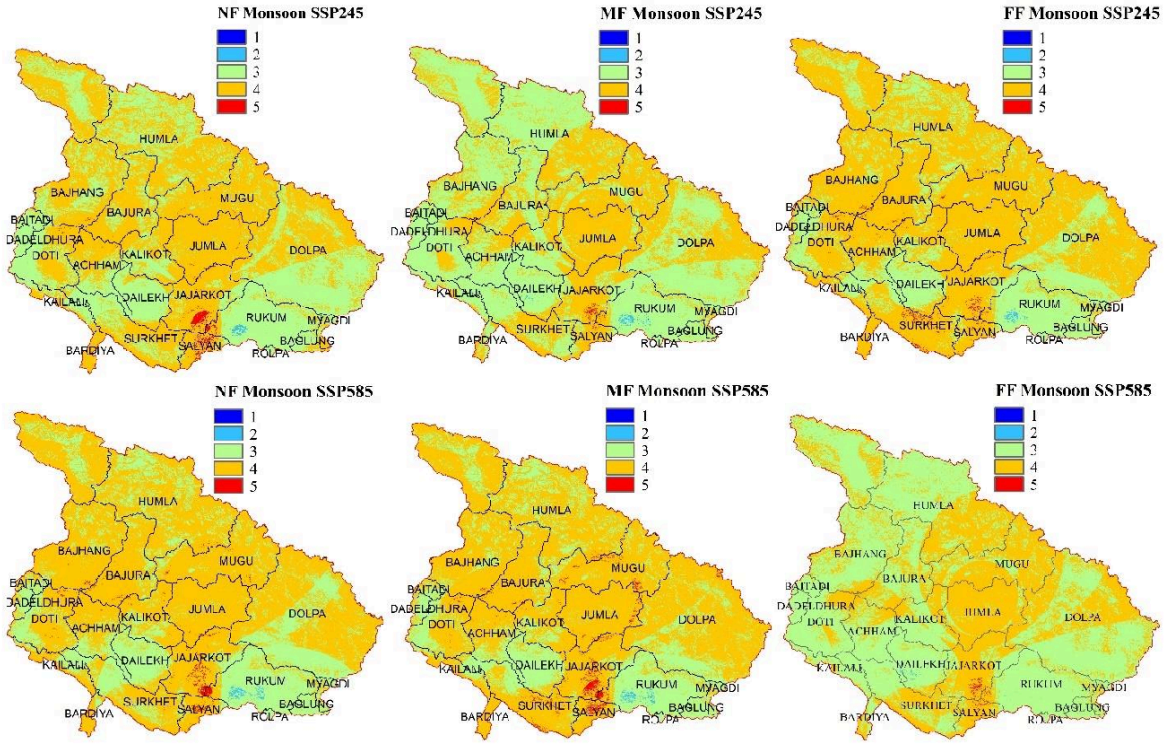


Figure 10: Monsoon DVM under SSP245 & SSP585 for NF, MF and FF

Figure 10

See image above for figure legend

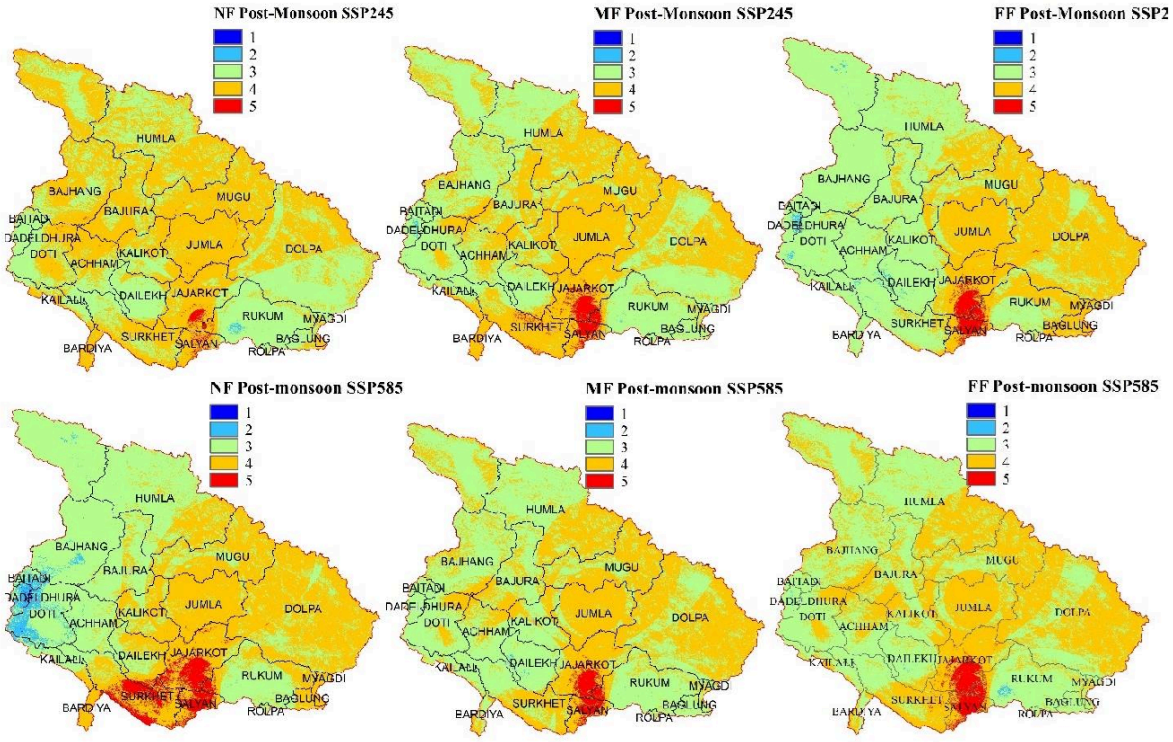


Figure 11: Post-Monsoon DVM under SSP245 & SSP585 for NF, MF and FF

Figure 11

See image above for figure legend

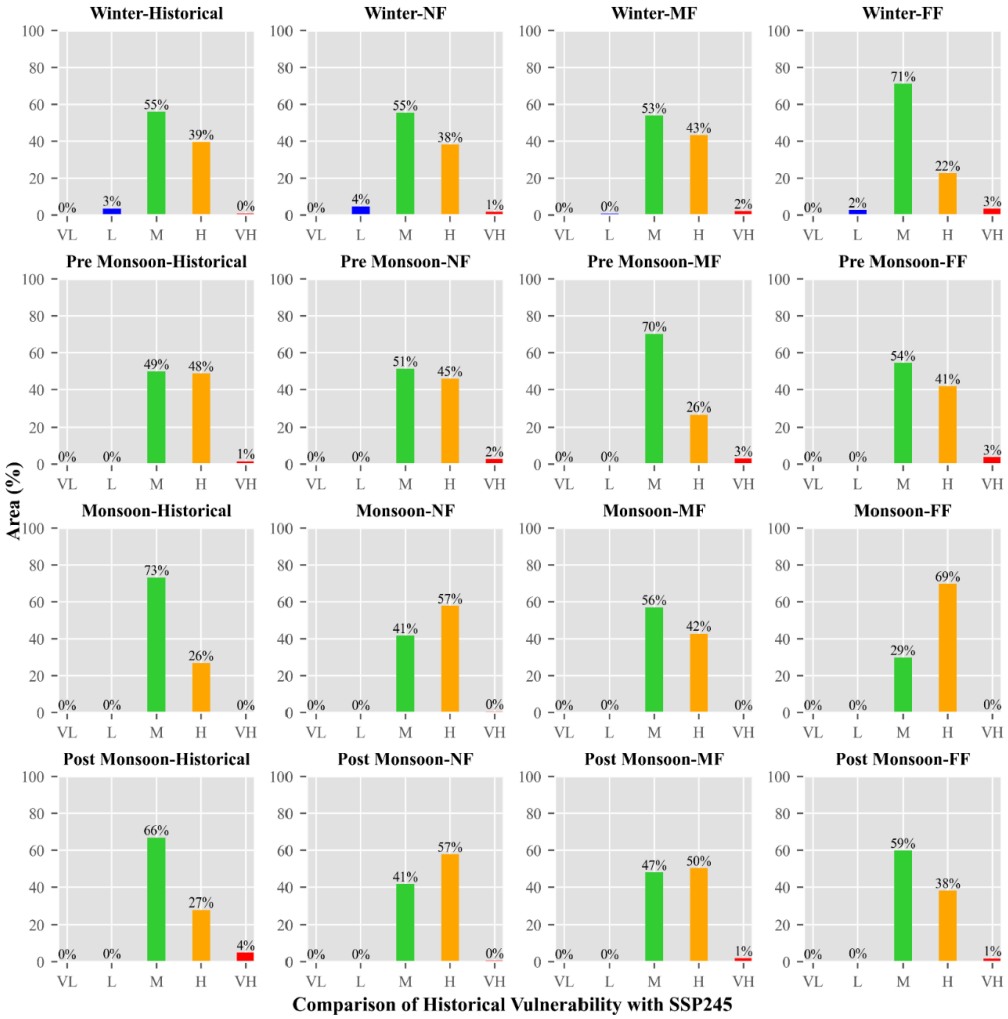


Figure 12: Comparison of Historical DVM with Future DVM prepared under SSP245

Figure 12

See image above for figure legend

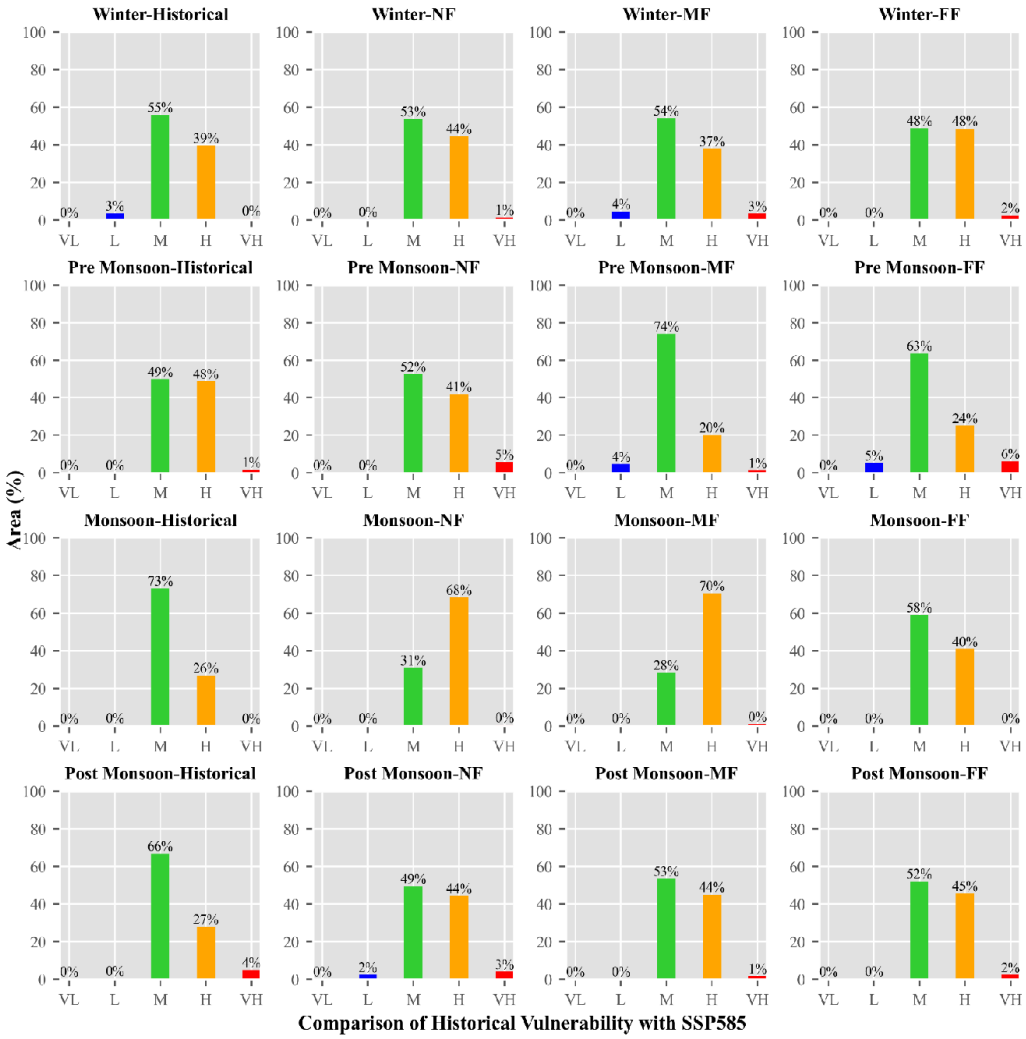


Figure 13: Comparison of Historical DVM with Future DVM prepared under SSP585

Figure 13

See image above for figure legend

Supplementary Files

This is a list of supplementary files associated with this preprint. Click to download.

- Additionalinformation.docx